

# Nonlinear Model Predictive Control of Permanent Magnet Synchronous Generators in DC Microgrids

Luis Herrera, Chad Miller, and Bang-Hung Tsao

**Abstract**—A new strategy is proposed to control interior permanent magnet generators in dc microgrids interfaced through an active rectifier. The controller design is based on the decomposition of the system dynamics into slow and fast modes using singular perturbation theory. An inner current controller is developed based on output regulation techniques and an outer voltage controller is proposed using Nonlinear Model Predictive Control (NMPC). The NMPC regulates the dc bus voltage and minimizes the ac side losses. Simulation results are then presented based on realistic conditions for aircraft power systems.

## I. INTRODUCTION

Electric machines play a fundamental role in the development of dc microgrids, with applications in the transportation industry. In electric vehicles, Permanent Magnet Synchronous Machines (PMSM) are a popular choice for the primary motor/generator [3]. In the More Electric Aircraft (MEA), these machines can be used for generation and motoring applications (e.g. actuators, propellers, etc.) [10], [11].

Control techniques for PMSMs used in motor drives generally ensure their optimal operation (in terms of efficiency) using techniques such as Maximum Torque per Amp (MTPA) and Maximum Torque per Volt (MTPV) [17]. These optimal conditions are relatively straightforward to implement in Surface Mounted PMSM (SPMSM), since the torque production only involves the permanent magnet and the q-axis current. Therefore, for a SPMSM in motoring mode, the q-axis current is used primarily to track a certain speed or torque reference during normal operation. In generator mode, this same current can be used to regulate the dc bus voltage [7].

However, the controllers of Interior PMSMs (IPMSM) based motors/generators do not always operate optimally. The main reason is that IPMSM machines can produce torque through both its permanent magnets and through the reluctance torque, due to the saliency of the rotor. Since the latter utilizes both d and q axis currents, when the same strategy as SPMSM is used for IPMSM, the reluctance torque is not optimally used and the generator/motor is operated at a lower power factor (increasing ac side losses). For example, in [2], [4], [6], [7], [9], [10], [16], [20], the q axis current is used to control the dc bus voltage (generator) and

speed/torque (motoring), irrespective of the type of machine used (SPMSM or IPMSM).

Most controllers for dc/ac and dc/dc converters employ a two loop strategy: inner current control and outer voltage or speed/torque control [12], [22], [23], and their stability analysis is typically presented using linearization techniques such as root locus [19]. This particular control structure owes its development to the nature of the physical system, composed of both fast and slow states. However, the (nonlinear) stability analysis and controller design for these types of controllers exploiting these fast/slow time constants has not been conducted. Nevertheless, singular perturbation techniques have been employed for power electronics and motor drives [14], [15], [21]. However, this type of control design does not generally follow an inner/outer loops and instead uses a composite control, i.e. a summation of two terms: the slow and fast components.

In this paper, we analyze the dynamics of PMSMs based generators for dc power systems using singular perturbation techniques and develop a controller which maintains the existing inner/outer loop control structure typically used in power electronics. In Section II, the overall generator dynamics with an active rectifier is presented along with an overview of the control procedure. In Section III, the inner current controller is developed using output regulation theory to track the desired reference. In Section IV, the outer controller is proposed using Nonlinear Model Predictive Control (NMPC) to achieve both voltage regulation and optimal operation of the machine. Simulation results are presented in Section V based on a BMW i3 IPMSMs in rectification mode (generator). Lastly, conclusion and future work are discussed.

The following notation is used throughout this paper. For a general matrix  $M \in \mathbb{R}^{n \times m}$ , its  $(i, j)$  element is denoted as  $M_{(i,j)}$ . The set of complex numbers with negative real part is denoted as  $C^-$ .

## II. PMSM BASED GENERATOR

An overview of a PMSM generator (PMSG) for dc microgrids is shown in Fig. 1. The overall dynamics are composed

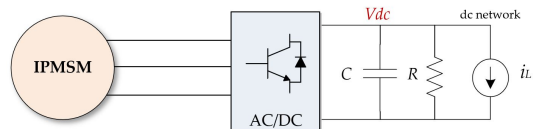


Fig. 1. PMSM based generator for dc microgrids.

of the ac side (PMSG) and dc side (capacitor) system. These systems can effectively be decomposed into fast and slow modes.

### A. System Dynamics

The dynamics of a PMSG with an active rectifier in rotor reference frame are given as follows [9], [17]:

$$\text{(dc)} \begin{cases} \dot{v}_{dc} = -\frac{1}{RC}v_{dc} + \frac{3}{2C}\frac{1}{v_{dc}}(v_d i_d + v_q i_q) - \frac{1}{C}i_L \end{cases} \quad (1)$$

$$\text{(ac)} \begin{cases} \dot{i}_d = \frac{-R_s}{L_d}i_d + \omega_r \frac{L_q}{L_d}i_q + \frac{1}{L_d}v_d \\ \dot{i}_q = \frac{-R_s}{L_q}i_q - \omega_r \frac{L_d}{L_q}i_d - \frac{\omega_r}{L_q}\lambda_m + \frac{1}{L_q}v_q \end{cases} \quad (2)$$

where  $i_d$  and  $i_q$  are the d and q axis current respectively,  $L_d$  and  $L_q$  are the inductances in the respective axis,  $R_s$  is the stator resistance,  $\omega_r$  is the rotor electrical frequency,  $\lambda_m$  is the permanent magnet flux linkage,  $C$  is the dc side capacitance,  $R$  is the parallel dc side resistance, and  $i_L$  is the dc side load current. The overall system was derived using the standard dq-transformation shown in the appendix.

The inputs to (1)-(2),  $v_d$  and  $v_q$ , can be written in terms of the modulation indices  $d_d, d_q \in [-1, 1]$ :

$$\begin{aligned} v_d &= d_d \frac{v_{dc}}{2} \\ v_q &= d_q \frac{v_{dc}}{2} \end{aligned} \quad (3)$$

based on sine PWM, coupling the dc voltage to the ac currents.

The system model, (1)-(2), can then be decomposed into fast and slow modes and written using singular perturbation theory as follows [15]:

$$\dot{x} = f(x, z, u, d) \quad (4)$$

$$\mu \dot{z} = g(x, z, u, d) \quad (5)$$

where  $0 < \mu \ll 1$ ,  $x \triangleq v_C$  and  $z \triangleq (i_d, i_q)^T$  are the slow and fast modes respectively,  $u = (d_d, d_q)^T$  are the inputs, and  $d \triangleq i_L$  is the disturbance.

### B. Overall Controller Design

The goal of a PMSG controller is to regulate the dc bus voltage. Typical controller design using singular perturbation theory decomposes the inputs into slow and fast components as  $u = u_s + u_f$ , generally known as composite control [15]. However, following existing approaches for control of electric machines [9] and power electronics [22], the controller will be developed as follows:

- The fast modes are regulated through  $u$  to follow a desired reference, i.e.  $z \rightarrow z^*$
- The slow modes are controlled through  $z^*$  to follow a certain reference, i.e.  $x \rightarrow x^*$

1) *Inner Loop*: For the fast mode controller design, the slow modes,  $x$ , are assumed to be constant, i.e.  $x = \bar{x}$ , and thus (5) can be written as:

$$\mu \dot{z} = g(\bar{x}, z, u, d) = \tilde{g}(z, u, d) \quad (6)$$

where  $u$  is designed by a static or dynamic controller to ensure fast regulation:  $z \rightarrow z^*$ .

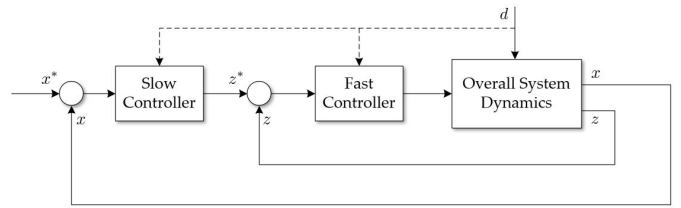


Fig. 2. Overview of the proposed controller design for singular perturbation systems. The dashed lines depends on the type of controller used and sensor availability.

2) *Outer Loop*: The outer/slow controller assumes that the dynamics of the closed loop fast subsystem are instantaneous:

$$0 = g(x, z, u, d) \quad (7)$$

and  $u$  can be obtained from (7) and written as a function of the slow and fast modes, i.e.  $u = p(x, z, d)$ . The slow subsystem then becomes:

$$\dot{x} = f(x, z, p(x, z, d), d) = \tilde{f}(x, z^*, d) \quad (8)$$

with the new input  $z^*$ .

Fig. 2 presents an overview of the proposed controller design. As can be inferred from this figure, the closed loop dynamics for the fast subsystem  $z$  need to be much faster than  $x$ . Therefore, fast regulation of  $z \rightarrow z^*$  is a crucial requirement.

### III. FAST INNER CURRENT REGULATOR

In this section, the controller design for the fast subsystem defined by (2) is presented. Following the procedure outlined in Section 1B, the slow mode (dc bus voltage) is assumed to be constant, i.e.  $v_{dc} = \bar{v}_{dc}$ . Therefore, the inputs/modulation indices,  $d_d$  and  $d_q$ , can be re-written in terms of the voltages  $v_d$  and  $v_q$  respectively based on (3). In this case, (2) becomes a linear state space system.

We consider standard decoupling techniques for inverters [9] by defining new inputs,  $\tilde{v}_d, \tilde{v}_q$ , as follows:

$$v_d = \tilde{v}_d - \omega_r L_q i_q \quad (9)$$

$$v_q = \tilde{v}_q + \omega_r L_d i_d + \omega_r \lambda_m$$

Plugging (9) into (2) we can obtain the following:

$$\dot{i}_d = \frac{-R_s}{L_d}i_d + \frac{1}{L_d}\tilde{v}_d \quad (10)$$

$$\dot{i}_q = \frac{-R_s}{L_q}i_q + \frac{1}{L_q}\tilde{v}_q \quad (11)$$

Therefore, each current controller can be designed independently. The controllers' goals are to regulate  $z \rightarrow z^*$  or  $i_d \rightarrow i_d^*$  and  $i_q \rightarrow i_q^*$ .

### A. D Axis Current Control

For the  $d$  axis current controller, we assume that the overall system, including the reference  $i_d^*$  (constant), is defined by the following linear dynamics:

$$\begin{aligned} \dot{i}_d &= \frac{-R_s}{L_d}i_d + \frac{1}{L_d}\tilde{v}_d & \dot{x}_d &= A_d x_d + B_d u_d \\ \dot{i}_d^* &= 0 & \Rightarrow \dot{x}_d^* &= S_d x_d^* \\ e_d &= -i_d + i_d^* & e_d &= C_d x_d + Q_d x_d^* \end{aligned} \quad (12)$$

The controller,  $u_d$ , is designed using output regulation techniques [8]:

$$u_d = K_d \xi_d + T_d x_d^* \quad (13)$$

where  $\xi_d$  is an estimate of  $x_d$  (e.g. using a Luenberger or Kalman filter),  $K_d$  is designed such that  $\sigma(A_d + B_d K_d) \subset \mathbb{C}^-$  and  $T_d$  is a feed forward gain satisfying:

$$\begin{aligned} A_d \Pi_d + B_d (K_d \Pi_d + T_d) &= \Pi_d S_d \\ C_d \Pi_d + Q_d &= 0. \end{aligned} \quad (14)$$

*Proposition 1:* The control law,  $u_d = K_d \xi_d + T_d x_d^*$ , satisfying (14) and  $\sigma(A_d + B_d K_d) \subset \mathbb{C}^-$  ensures  $i_d \rightarrow i_d^*$ . The proof follows standard arguments of output regulation theory [8].

### B. Q Axis Current Control

A similar procedure is followed for the  $q$ -axis current regulator. The overall dynamics are as follows:

$$\begin{aligned} \dot{i}_q &= \frac{-R_s}{L_q} i_q + \frac{1}{L_q} \tilde{v}_q & \dot{x}_q &= A_q x_q + B_q u_q \\ \dot{i}_q^* &= 0 & \dot{x}_q^* &= S_q x_q^* \\ e_q &= -i_q + i_q^* & \dot{e}_q &= C_q x_q + Q_q x_q^* \end{aligned} \quad (15)$$

and the goal is to ensure that  $i_q \rightarrow i_q^*$  or  $e_q \rightarrow 0$  as  $t \rightarrow \infty$ . The controller law is  $u_q$  is given in a similar form:

$$u_q = K_q \xi_q + T_q x_q^* \quad (16)$$

where  $\xi_q$  is an estimate of the current  $i_q$  through a linear observer. The feedback matrix  $K_q$  is designed to ensure that  $\sigma(A_q + B_q K_q) \subset \mathbb{C}^-$  and  $T_q$  satisfies the same full information regulator equations:

$$\begin{aligned} A_q \Pi_q + B_q (K_q \Pi_q + T_q) &= \Pi_q S_q \\ C_q \Pi_q + Q_q &= 0. \end{aligned} \quad (17)$$

*Proposition 2:* The control law  $u_q = K_q \xi_q + T_q x_q^*$  satisfying  $\sigma(A_q + B_q K_q) \subset \mathbb{C}^-$  and (17) ensures  $i_q \rightarrow i_q^*$  as  $t \rightarrow \infty$ .

Lastly, the feedback matrices  $K_d$  and  $K_q$  should be optimized carefully in order to guarantee that fast regulation of the currents  $i_d$  and  $i_q$ . Semi-definite Programming (SDP) techniques are used in the case study section for the tuning of the controller gains [13].

## IV. NMPC BASED DC VOLTAGE CONTROL - SLOW SUBSYSTEM

NMPC is used for the controller design of the slow subsystem,  $v_{dc}$ , in order to provide the references  $i_d^*$ ,  $i_q^*$  to the inner current control. In this case, it is assumed that the fast dynamics are instantaneous, i.e.  $\mu \rightarrow 0$  in (5). Based on (2), the left hand side is simplified as:

$$\begin{aligned} 0 &= \frac{-R_s}{L_d} i_d + \omega_r \frac{L_q}{L_d} i_q + \frac{1}{L_d} v_d \\ 0 &= \frac{-R_s}{L_q} i_q - \omega_r \frac{L_d}{L_q} i_d - \frac{\omega_r}{L_q} \lambda_m + \frac{1}{L_q} v_q \end{aligned} \quad (18)$$

and  $v_d$  and  $v_q$  can be obtained as:

$$\begin{aligned} v_d &= -r_s i_d + \omega_r L_q i_q \\ v_q &= -r_s i_q - \omega_r L_d i_d - \omega_r \lambda_m \end{aligned} \quad (19)$$

Plugging (19) into the dc voltage dynamics (1), the following nonlinear system is derived:

$$\begin{aligned} \dot{v}_{dc} &= -\frac{1}{RC} v_{dc} - \frac{1}{C} i_L \\ &+ \frac{3}{2C} \frac{1}{v_{dc}} (-r_s (i_d^2 + i_q^2) + \omega_r (L_q - L_d) i_q i_d - \omega_r \lambda_m i_q) \end{aligned} \quad (20)$$

Notice that the inputs in this case are now  $i_d = i_d^*$  and  $i_q = i_q^*$ , i.e. the references for the inner loop controller. In addition, the new model (20) is nonlinear due to the second degree terms in the inputs and the reciprocal of the state term ( $1/v_{dc}$ ).

The goal of the slow subsystem controller is to regulate the dc bus voltage to a certain reference,  $v_{dc}^*$ , while at the same time reducing losses and satisfying constraints associated with the voltage boundaries (e.g. see MIL-STD-704F [1]) and the physical limits of the PMSG (current and voltage).

### A. Optimal Operation and Constraints

Since only active power is consumed by the dc side of a PMSG, the ac side currents should be controlled as to provide only active power whenever possible (i.e. unity power factor). The torque produced by the PMSG is defined as follows:

$$T_e = \frac{3P}{2} (\lambda_m i_q + (L_d - L_q) i_q i_d) \quad (\text{Nm}) \quad (21)$$

where  $P$  is the number of poles. Therefore, the electrical power, at the ac/mechanical side, can be obtained from the previous equation using the torque/power relation:

$$\begin{aligned} P_e &= T_e \omega_m = \frac{3P}{2} \omega_m (\lambda_m i_q + (L_d - L_q) i_q i_d) \\ \Rightarrow P_e &= \frac{3}{2} \omega_r (\lambda_m i_q + (L_d - L_q) i_q i_d) \end{aligned} \quad (22) \quad (23)$$

where  $\omega_m$  is the rotor mechanical speed (rad/sec) and the last equation is obtained from  $\omega_r = \frac{P}{2} \omega_m$ .

For generation mode, the electrical power is decided only by the dc load. However, since  $P_e$  is a function of both  $i_d$  and  $i_q$ , there are multiple solutions to (23). The optimal solution minimizes the rms (or peak) of the ac side currents, i.e. providing only active power whenever possible.

The constraints for a PMSG typically involve current and voltage limits. These can be written as follows:

$$i_d^2 + i_q^2 \leq I_{\text{peak}}^2 \quad (24)$$

$$v_d^2 + v_q^2 \leq V_{\text{peak}}^2 \quad (25)$$

Plugging (19) into (25) and assuming  $r_s \approx 0$ , we can rewrite the voltage constraints in terms of  $dq$  currents:

$$(\omega_r L_q i_q)^2 + (\omega_r L_d i_d + \omega_r \lambda_m)^2 \leq V_{\text{peak}}^2 = \left(\frac{v_{dc}}{2}\right)^2 \quad (26)$$

The equality  $V_{\text{peak}}^2 = \left(\frac{v_{dc}}{2}\right)^2$  is based on sine PWM as shown in (3) for  $d_q = d_d = 1$ .

Finally, the optimal operation of the PMSM based generator for a fixed dc load power,  $P_e$ , is a solution of the following optimization problem:

$$\begin{aligned} \min_{i_d, i_q} \quad & i_d^2 + i_q^2 \\ \text{s.t.} \quad & \frac{3}{2}\omega_r (\lambda_m i_q + (L_d - L_q)i_q i_d) = P_e \\ & i_d^2 + i_q^2 \leq I_{\text{peak}}^2 \\ & (\omega_r L_q i_q)^2 + (\omega_r L_d i_d + \omega_r \lambda_m)^2 \leq \left(\frac{v_{dc}}{2}\right)^2 \end{aligned} \quad (27)$$

During steady state operation, the slow side controller should satisfy (27). Of particular importance are the non-trivial solutions for (27), contained in the interior of the following set:

$$\mathcal{E} = \left\{ (i_d, i_q)^T \in \mathbb{R}^2 \mid i_d^2 + i_q^2 \leq I_{\text{peak}}^2, \right. \\ \left. (\omega_r L_q i_q)^2 + (\omega_r L_d i_d + \omega_r \lambda_m)^2 \leq \left(\frac{v_{dc}}{2}\right)^2 \right\} \quad (28)$$

i.e. when the inequalities in (27) are non-binding. For this case, it is possible to supply only active power from the generator, hence minimizing the ac currents.

### B. NMPC Formulation

We consider a NMPC controller for dc bus voltage regulation and optimal operation of the PMSG. To ensure convergence to the desired reference voltage, we expand (20) by an integral term as follows:

$$\begin{aligned} \dot{v}_{dc} &= -\frac{1}{RC}v_{dc} - \frac{1}{C}i_L \\ &+ \frac{3}{2C} \frac{1}{v_{dc}} (-r_s(i_d^2 + i_q^2) + \omega_r(L_q - L_d)i_q i_d - \omega_r \lambda_m i_q) \\ \dot{e}_{\text{int}} &= -v_{dc} + v_{dc}^* \end{aligned} \quad (29)$$

For simplicity, (29) is written as the nonlinear system:

$$\dot{x} = f_c(x, u, d) \quad (30)$$

where  $x = (v_{dc}, e_{\text{int}})^T$ ,  $u = (i_d, i_q)^T$ ,  $d = i_L$ .

The extended nonlinear system (29) is then discretized at a certain time step  $T_s$ :

$$x_{k+1} = f_d(x_k, u_k, d_k) \quad (31)$$

using Forward Euler (FE). The NMPC can now be formally stated:

$$\begin{aligned} \min_{x_k, u_k} \quad & \sum_{k=0}^{N-1} (x_k - x_{\text{ref}})^T Q (x_k - x_{\text{ref}}) + u_k^T R u_k + \\ & (x_N - x_{\text{ref}})^T Q (x_N - x_{\text{ref}}) \\ \text{s.t.} \quad & \begin{cases} x_{k+1} = f_d(x_k, u_k, d_k) \\ \|u_k\|_2^2 \leq I_{\text{peak}}^2 \quad \text{for } k = 0, \dots, N-1 \\ (\omega_r L_q u_{2,k})^2 + (\omega_r L_d u_{1,k} + \omega_r \lambda_m)^2 \leq \left(\frac{x_{1,k}}{2}\right)^2 \\ V_{\text{dc-min}} \leq x_{1,k} \leq V_{\text{dc-max}} \quad \text{for } k = 1, \dots, N \end{cases} \end{aligned} \quad (32)$$

where  $N$  is the prediction horizon,  $x_{\text{ref}} = (v_{dc}^*, 0)^T$ , and  $Q, R \succ 0$ . The main advantage of using the proposed NMPC is that under certain conditions, the optimal solution to (32) satisfies (27) during steady state, as shown in the following proposition.

*Proposition 3:* Assume  $Q = \text{Diag}(\gamma, \beta)$  and  $R = \gamma I$ , where  $\epsilon, \gamma, \beta$  are positive constants. Let  $P_e \triangleq - (v_{dc}^2/R + v_{dc}i_L)$ ,  $r_s = 0$ , and perfect tracking is achieved, i.e.  $x_{1,k} = v_{dc}^*$  for  $k$  greater than a certain  $M$ .

During steady state ( $x_{k+1} = x_k$ ), assume the optimal solution to (32) is as follows:  $X^* = x_k^* \otimes \mathbf{1}_N^T$  and  $U^* \triangleq u_k^* \otimes \mathbf{1}_N^T$ , where  $N$  is the horizon. Then  $u_k^*$  is also a solution to (27).

*Proof:* During steady state, the optimal solution of the MPC problem satisfies:

$$x_k^* = x_k^* + T_s f_c(x_k^*, u_k^*, d_k) \quad (\text{using FE}) \quad (33)$$

Using (29), the previous equation simplifies to:

$$-\left(\frac{v_{dc}}{R} + i_L\right) = \frac{3}{2} \frac{1}{v_{dc}} (\omega_r(L_d - L_q)i_q i_d + \omega_r \lambda_m i_q) \quad (34)$$

Multiplying both sides of (34) by  $v_{dc}$  we obtain:

$$P_e = -\left(\frac{v_{dc}^2}{R} + v_{dc}i_L\right) = \frac{3}{2}\omega_r (\lambda_m i_q + (L_d - L_q)i_q i_d) \quad (35)$$

Therefore, the same equality constraint of (27) is obtained by the previous equation. Lastly, since  $R = \gamma I$  implies that  $u_k^T R u_k = \gamma \|u_k\|_2^2$ , during steady state the cost function (besides  $\gamma$ ) and constraints of (32) are equivalent to (27). Therefore, the solution  $u_k^*$  for (32) during steady state is also a solution to (27). ■

The proposed control strategy not only dynamically regulates  $v_{dc}$  to the reference voltage, but also optimizes the steady state based on (27). During high speed operation, it may not always be possible to be in the interior of  $\mathcal{E}$  and

TABLE I. PMSM parameters based on the BMW i3 motor/generator [5], [18].

$L_d$	0.090 mH	$L_q$	0.255 mH	$\lambda_m$	0.0385 Vs
$r_s$	5.3 mΩ	$n_{\text{max}}$	11400 rpm	Poles	12
$T_{\text{max}}$	250 Nm	$P_{\text{max}}$	125 kW	$I_{\text{phase-peak}}$	400 A

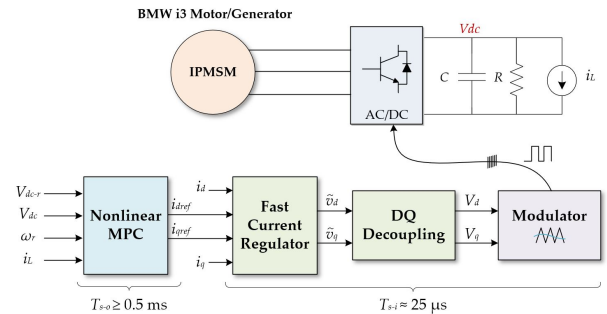
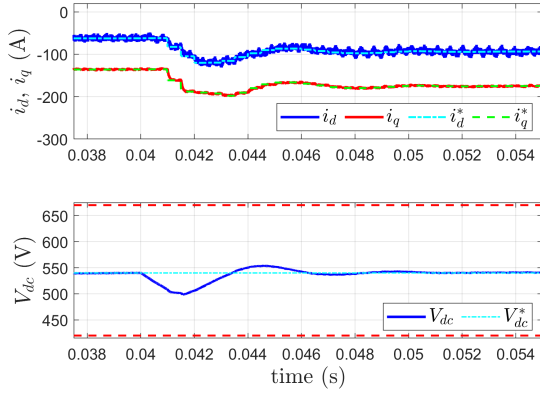
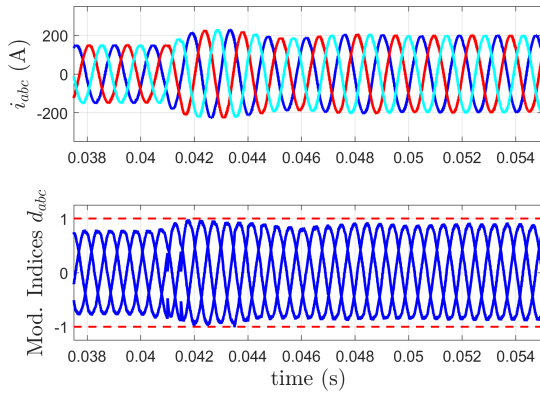


Fig. 3. Proposed control strategy for a IPMSM based generator system in dc microgrids.



(a)  $DQ$  currents (top) and dc bus voltage (bottom). The dashed lines represent the references.



(b) Three phase currents (top) and modulation indices in  $abc$  form (bottom).

Fig. 4. Simulation results for case 1. A load change from 43.5 kW to 62.25 kW occurs at  $t = 0.04$  s.

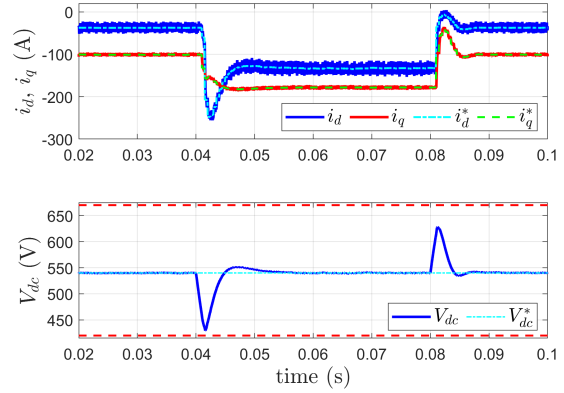
TABLE II. Control parameters for active rectification of an IPMSM based generator.

$F_{sw}$ (switching freq.)	40 kHz	$T_{s-o}$	0.5 ms
$T_{s-i}$	25 $\mu$ s	$V_{dc-min}$	420 V
$V_{dc-max}$	670 V	N	10
$Q$	Diag(0.1, 9000)	$R$	$0.1I_{2 \times 2}$

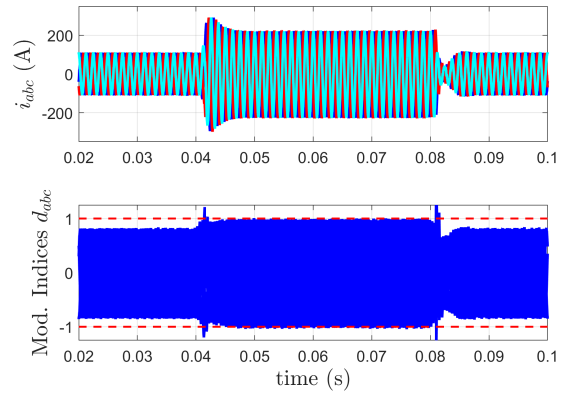
flux weakening is implicitly achieved by ensuring the current and voltage limits in  $\mathcal{E}$  are satisfied.

## V. CASE STUDY AND SIMULATION RESULTS

We consider the parameters for the IPMSM shown in Tab. I. These machine parameters are based on the BMW i3 motor/generator [5], [18]. The voltage reference is set to 540 V with a maximum load of 125 kW. The NMPC discretization rate is at least  $T_{s-o} \geq 0.5$  ms while the inner loop current regulator sampling time is  $T_{s-i} = 25$   $\mu$ s (corresponding to a  $F_{sw} = 40$  kHz switching frequency). The overall control strategy is shown in Fig. 3. As can be seen in this figure, the NMPC is the outer control associated with the slow subsystem ( $v_{dc}$ ), with inputs as the reference  $dq$  currents to be used in the fast current regulator. The  $dq$



(a)  $DQ$  currents (top) and dc bus voltage (bottom). The dashed lines represent the references.



(b) Three phase currents (top) and modulation indices in  $abc$  form (bottom).

Fig. 5. Simulation results for case 2. A pulsed load occurs at  $t = 0.04$  s (on) and  $t = 0.08$  s (off). The load changes from 34 kW to 81 kW.

decoupling block is based on equations (10) and (11). Finally, the modulator uses (3) to compute the modulation indices for sine PWM. The control parameters are summarized in Tab. II.

### A. Case 1

We first consider the parameters in Tab. II with a dc load change from 43.5 kW to 62.25 kW at  $t = 0.04$  s. The mechanical speed of the machine is  $n = 7000$  rpm. The optimal currents at 43.5 kW can be solved using (27) as  $i_{d-opt} = -62$  A and  $i_{q-opt} = -135.3$ , while at 62.25 kW are  $i_{d-opt} = -93.5$  A and  $i_{q-opt} = -174.9$  A. The steady state values for the  $dq$  currents are optimal for both of these power levels, as can be seen from Fig. 4a. In addition, the reference currents are tracked accurately and much faster than the NMPC sampling time. The dc bus voltage is regulated within 10 ms and is maintained within the bounds (dashed red).

Fig 4b shows the phase currents and the modulation indices ( $abc$ ). Both of these can be obtained using the inverse Park transformation:

$$I_{abc} = K^{-1}(i_d, i_q, 0)^T \text{ and } d_{abc} = K^{-1}(d_d, d_q, 0)^T \quad (36)$$

where  $K$  is defined in the appendix. As mentioned previously,  $d_d, d_q \in [-1, 1]$  for sine PWM, which is implicitly enforced through (26).

### B. Case 2

Next, we consider a pulsed load change from 34 kW to 81 kW at  $t = 0.04$  s and  $t = 0.08$  s (on/off respectively). The mechanical speed in this case is  $n = 8000$  rpm. The control parameters are the same as the previous case. Fig. 5a shows the  $dq$  currents and the dc bus voltage. It can be seen that the voltage is kept within its limits and converges to the reference of 540 V. Fig. 5b shows the phase currents and the modulation signals. It can be seen that when the load is set to 81 kW, the modulation indices reach their limit of  $\pm 1$ . This implies that inequality (26) is binding at this load power. In this mode of operation, more  $i_d$  current is added to reduce the effect of the permanent magnet flux linkage and its induced back emf.

## VI. CONCLUSION AND FUTURE WORK

A controller design is presented for PMSG in dc microgrids. The proposed method is analyzed using similar assumptions of singular perturbation theory. The inner loop controller for the ac currents is developed using output regulation while the outer loop control for the dc bus voltage tracking is based on NMPC. It is shown that the NMPC is able to track the dc bus voltage accurately and minimize the peak ac currents, increasing efficiency. Simulation results are presented using parameters for the BMW i3 IPMSM. Future work includes full hardware testing of the proposed controller and stability analysis of the proposed techniques.

## VII. ACKNOWLEDGEMENT

This research was supported by the AFRL Summer Faculty Fellowship Program (SFFP). Distribution A: approved for public release, distribution unlimited. Case Number: 88ABW-2020-2970.

## APPENDIX

The abc to dq transformation used in the derivation of (1) and (2) is the following:

$$K = \frac{2}{3} \begin{pmatrix} \cos(\theta_r) & \cos(\theta_r - 2\pi/3) & \cos(\theta_r + 2\pi/3) \\ -\sin(\theta_r) & -\sin(\theta_r - 2\pi/3) & -\sin(\theta_r + 2\pi/3) \\ \frac{1}{2} & \frac{1}{2} & \frac{1}{2} \end{pmatrix} \quad (37)$$

## REFERENCES

- [1] MIL-STD-704F, *Aircraft Electric Power Characteristics*. Military Standard.
- [2] S. Bozhko, M. Rashed, C. I. Hill, S. S. Yeoh, and T. Yang. Flux-weakening control of electric starter-generator based on permanent-magnet machine. *IEEE Transactions on Transportation Electrification*, 3(4):864–877, 2017.
- [4] N. Clements, G. Venkataramanan, and T. M. Jahns. Design considerations for a stator side voltage regulated permanent magnet ac generator. In *2009 IEEE Energy Conversion Congress and Exposition*, pages 2763–2770, 2009.

- [3] K. T. Chau, C. C. Chan, and C. Liu. Overview of permanent-magnet brushless drives for electric and hybrid electric vehicles. *IEEE Transactions on Industrial Electronics*, 55(6):2246–2257, 2008.
- [5] G. Dajaku, H. Zhou, X. Dajaku, and D. Gerling. Novel rotor design with reduced rare-earth material for pm machines. In *2019 IEEE International Electric Machines Drives Conference (IEMDC)*, pages 1–7, 2019.
- [6] H. Dehghani Tafti, A. I. Maswood, Z. Lim, G. H. P. Ooi, and P. H. Raj. Proportional-resonant controlled npc converter for more-electric-aircraft starter-generator. In *2015 IEEE 11th International Conference on Power Electronics and Drive Systems*, pages 41–46, 2015.
- [7] L. Fan, T. Yang, M. Rashed, and S. Bozhko. Sensorless control of dual-three phase pmsm based aircraft electric starter/generator system using model reference adaptive system method. In *CSAA/IET International Conference on Aircraft Utility Systems (AUS 2018)*, pages 787–794, 2018.
- [8] B. A. Francis. The linear multivariable regulator problem. *SIAM Journal on Control and Optimization*, 15(3):486–505, 1977.
- [9] F. Gao and S. Bozhko. Modeling and impedance analysis of a single dc bus-based multiple-source multiple-load electrical power system. *IEEE Transactions on Transportation Electrification*, 2(3):335–346, 2016.
- [10] F. Gao, X. Zheng, S. Bozhko, C. I. Hill, and G. Asher. Modal analysis of a pmsg-based dc electrical power system in the more electric aircraft using eigenvalues sensitivity. *IEEE Transactions on Transportation Electrification*, 1(1):65–76, 2015.
- [11] P. Giangrande, V. Madonna, G. Sala, A. Kladas, C. Gerada, and M. Galea. Design and testing of pmsm for aerospace ema applications. In *IECON 2018 - 44th Annual Conference of the IEEE Industrial Electronics Society*, pages 2038–2043, Oct 2018.
- [12] L. Herrera, E. Inoa, F. Guo, J. Wang, and H. Tang. Small-signal modeling and networked control of a phev charging facility. *IEEE Transactions on Industry Applications*, 50(2):1121–1130, 2014.
- [13] L. Herrera, W. Zhang, and J. Wang. Stability analysis and controller design of dc microgrids with constant power loads. *IEEE Transactions on Smart Grid*, 8(2):881–888, March 2017.
- [14] J. W. Kimball and P. T. Krein. Singular perturbation theory for dc–dc converters and application to pfc converters. *IEEE Transactions on Power Electronics*, 23(6):2970–2981, 2008.
- [15] P. Kokotović, H. K. Khalil, and J. O’reilly. *Singular perturbation methods in control: analysis and design*. SIAM, 1999.
- [16] D. Miao, Y. Mollet, J. Gyselinck, and J. Shen. Dc voltage control of a wide-speed-range permanent-magnet synchronous generator system for more electric aircraft applications. In *2016 IEEE Vehicle Power and Propulsion Conference (VPPC)*, pages 1–6, 2016.
- [17] K. H. Nam. *AC motor control and electrical vehicle applications*. CRC press, 2018.
- [18] B. Ozpineci. Oak ridge national laboratory annual progress report for the electric drive technologies program. Technical report, Oak Ridge National Lab.(ORNL), Oak Ridge, TN (United States), 2016.
- [19] N. Pogaku, M. Prodanovic, and T. C. Green. Modeling, analysis and testing of autonomous operation of an inverter-based microgrid. *IEEE Transactions on power electronics*, 22(2):613–625, 2007.
- [20] S. M. Tripathi, A. N. Tiwari, and D. Singh. Optimum design of proportional-integral controllers in grid-integrated pmsg-based wind energy conversion system. *International Transactions on Electrical Energy Systems*, 26(5):1006–1031, 2016.
- [21] F. Umbría, J. Aracil, F. Gordillo, F. Salas, and J. A. Sánchez. Three-time-scale singular perturbation stability analysis of three-phase power converters. *Asian Journal of Control*, 16(5):1361–1372, 2014.
- [22] J. C. Vasquez, J. M. Guerrero, M. Savaghebi, J. Eloy-Garcia, and R. Teodorescu. Modeling, analysis, and design of stationary-reference-frame droop-controlled parallel three-phase voltage source inverters. *IEEE Transactions on Industrial Electronics*, 60(4):1271–1280, 2012.
- [23] X. Wang, F. Blaabjerg, and W. Wu. Modeling and analysis of harmonic stability in an ac power-electronics-based power system. *IEEE Transactions on Power Electronics*, 29(12):6421–6432, 2014.